View metadata, citation and similar papers at core.ac.uk
brought to you by CORE
provided by Brunel University Research Archive

A Model for Uphill Droplet Motion

Felipe M. MANCIO REIS [1, 2], Pascal LAVIEILLE [1, 2], Marc MISCEVIC [1, 2 *]

* Corresponding author: Tel.: +33 (0)5 61 55 83 07; Fax: +33 (0)5 61 55 60 21;
Email: marc.miscevic@laplace.univ-tlse.fr
[1] Université de Toulouse, UPS, INPT, LAPLACE (Laboratoire Plasma et Conversion d'Energie),
118 route de Narbonne, F-31062, France
[2] CNRS, LAPLACE, F-31062 Toulouse, France

Abstract This paper focuses on the behaviour of a liquid droplet over the surface of a treated solid substrate. It deals with the use of surface tension forces induced by setting up a gradient of wettability to allow the evacuation of the dispersed phase. The main aim is to present a new model capable of predicting the motion of a droplet of known volume over a surface with a wettability gradient that explicitly takes contact angle hysteresis into account. Several authors have established a phenomenological footprint radius, from which the droplet starts moving. Our model, provides a relationship to find this critical droplet size. The results show that the contact angle hysteresis parameter appears to be a key issue in droplet dynamics and in the accurate prediction of droplet motion.

Keywords: wettability gradient, contact angle hysteresis, droplet hydrodynamics

1. Introduction

Two-phase systems are among the most efficient to exchange large heat fluxes. Latent heat associated with a change of state of matter, e.g. boiling, evaporation, vapour condensation, is the key to these two-phase systems. Nevertheless, they do require dealing with a dispersed phase. In microgravity for instance, the dispersed phase cannot be evacuated using a gravitational field. One possible way to evacuate the dispersed phase consists of using surface tension forces induced by a wettability gradient. These forces establish a mechanical disequilibrium in the embryos forming on the wall. The spreading of a liquid over a solid is controlled by the contact angle and the surface tension of each interface. Then, if the parameters do not have equilibrium values, a driving force arises to move the droplet from the more hydrophobic to the more hydrophilic regions.

The motion induced by the wettability gradient is complex and multi-scale. This phenomenon has been widely studied for several decades. Greenspan [1] was the first to report this method. Brochard [2] gave an analytical description using a hydrodynamic theory. The analyses involved a balance of local forces between the force at the contact line and the viscous force. Several years later, Chaudhury and Whitesides [3] demonstrated the phenomenon experimentally. They achieved upward motion of a 1 to 2 µL droplet on a 15º tilted plate with a wettability gradient. They found that a droplet speed of 1 to 2 mm/s was only possible with a contact angle hysteresis of less than 10º.

More recently, Moumen et al. [4] using the same chemical technique as Chaudhury and Whitesides, conducted a very thorough experimental campaign on the motion of tetraethylene glycol droplets of different volumes on three surfaces with different gradients. The authors established a model that took contact angle hysteresis into account using a phenomenological approach based on experimental results. They proposed an accommodating method to reduce the cosine of the contact angle around the periphery of the droplet. A critical footprint radius was then derived for which the droplets start moving.

In this paper, we propose a model that is explicitly related to contact angle hysteresis,

noted CAH hereafter. The motion of the droplet on such wettability gradients is directly induced by an imbalance of surface tension forces acting on the contact line region. However, setting the droplet in motion is strongly dependent on the CAH value, which tends to pin the triple line. The model presented in this paper describes droplet motion on any wettability gradient surface with CAH. It also manages to quantify hysteresis knowing the displacement of the drop and the surface wettability properties. An analysis of the model is also conducted to determine the critical footprint radius.

2. Dynamic model

A drop placed on a horizontal wettability gradient surface is subjected to two primary forces. The force generated by the surface energy gradient, i.e. driving force (F_θ), and the viscous force (F_μ), which naturally opposes the movement of the droplet and is directly related to its velocity. A gravitational force will also occur if the surface is inclined (at an angle α to the horizontal). The dynamic model presented hereafter is based on four main hypotheses:

i. the inertial term is ignored,
ii. the droplet maintains its spherical cap shape during movement, which means that the dynamic contact angle is the same everywhere around the periphery of the droplet,
iii. the volume of the droplet remains constant,
iv. the interface is always in its most stable form, i.e. minimum of surface energy.

Newton's first law on the x-axis, tangent to the wall is then written:

$$F_\theta(x_G,t) + F_\mu(x_G,t) - mg\sin\alpha = 0 \qquad (1)$$

where x_G is the center of mass of the droplet. As reported previously, the CAH may drastically change the expected trajectory of the droplet. In the following, some considerations about the CAH are highlighted before establishing the model itself using results reported by Moumen et al. [4].

2.1 Contact angle hysteresis

The CAH has been and remains a main interfacial phenomena issue. Indeed, assuming a smooth and homogeneous surface, Young [5] defined a unique equilibrium contact angle. Nevertheless, real surfaces are rough and may contain chemical impurities. Thus, in practice there is not a single equilibrium angle but a range of static angles distributed between the advancing (θ_a) and the receding (θ_r) contact angles. CAH is defined as the difference between the extreme values of static contact angles. As presented above, the main point of the model developed in this paper is that it explicitly takes the CAH into account. First, let us consider a drop on an inclined plate with homogeneous wettability. Because of CAH and the deformation of the interface, the drop starts sliding when the front and the rear contact angles reach the extreme values, θ_{aB} and θ_{rA} respectively (fig. 1):

$$\begin{cases} \theta_{front} > \theta_{aB} \\ \theta_{rear} < \theta_{rA} \end{cases}. \qquad (2)$$

However, considering small droplets (typically less than 1 µL), no deformation is obtained ($\theta_{rear} = \theta_{front}$). This unique angle along the periphery will be noted θ in the following (when the droplet moves, θ is the dynamic contact angle). So, small droplets do not slide on inclined surfaces with CAH whatever the inclination. Analogically, a small droplet placed on a wettability gradient surface is subjected to the same constraints regarding the hysteresis effect, but because of the wettability gradient, it is possible for the droplet to have a unique dynamic contact angle around the whole periphery and simultaneously satisfy Eq. 2. There are three ways to overcome the hysteresis effect with a wettability gradient. The first is simply to reduce the CAH. The second consists in increasing the volume, i.e. the footprint radius, of the droplet until it reaches a critical value permitting its motion. The last way to overcome the hysteresis effect is to create a sharper wettability gradient.

2.2 Driving force and viscous force

As previously stated, for small droplets the CAH plays a major role. Several driving force models exist in the literature but just a few consider the hysteresis effect. The difference between the static contact angle and the real contact angle at each point of the contact line causes disequilibrium of the Young forces. The total surface tension force without contact angle hysteresis is expressed as [4]:

$$F_\theta(x_G,t) = \gamma_{lv} R(x_G,t) \int_0^{2\pi} \left(\cos\theta_s(x) - \cos\theta(x_G,t)\right)\cos\phi d\phi \quad (3)$$

where $x = x_G + R(x_G, t)\cos\phi$, x_G is the abscissa of the centre of mass of the droplet, γ_{lv} is the liquid-vapour surface tension, θ_s is the static contact angle, θ is the real contact angle verifying the minimum surface energy, ϕ is the azimuthal angle, and R is the footprint radius of the droplet at the centre of mass x_G directly related to the real contact angle:

$$R(x_G,t) = \sin\theta(x_G,t)\left(3V/\pi\right)^{1/3} \left(2 - 3\cos\theta(x_G,t) + \cos^3\theta(x_G,t)\right)^{-1/3} \quad (4)$$

The spherical cap shape hypothesis implies that the cohesion force, generated by the Laplace-Young pressure difference at the liquid-vapour interface, is greater than the driving force. So the model is valid if the volume of the droplet satisfies the following condition,

$$F_\theta(x_G,t) << 4\pi\gamma_{lv} R(x_G,t)\frac{1-\cos\theta(x_G,t)}{\sin\theta(x_G,t)} \quad (5)$$

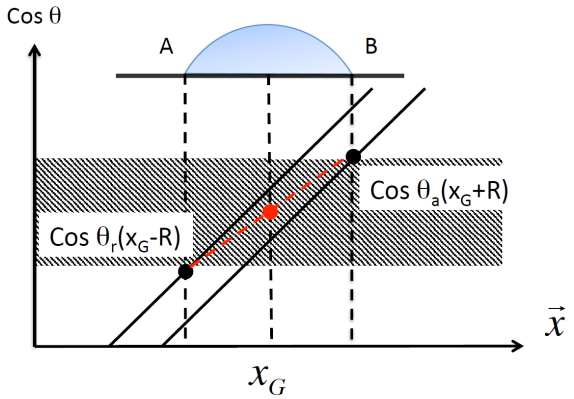

Fig. 1 The linear cosine between the advancing and receding contact angles.

To model a driving force taking into account the CAH, full knowledge of the real contact angle all around the periphery is necessary. Indeed, considering relation (2) the static contact angle varies continuously from the advancing contact angle at the front to the receding contact angle at the rear of the droplet. As the droplet is small, the cosine of the contact angle variation with the longitudinal location can be considered linear (see Fig. 1). Writing $\cos\theta_s(x, t) = a(x_G, t)x + b(x_G, t)$ and because the real contact angle remains the same everywhere at the periphery, its cosine integration is zero. Eq. 3 becomes then:

$$F_\theta(x_G,t) = \gamma_{lv} R(x_G,t) \int_0^{2\pi} \left(a(x_G,t)(R(x_G,t)\cos\phi + x_G) + b(x_G,t)\right)\cos\phi d\phi. \quad (6)$$

The parameter $a(x_G, t)$ represents the slope of the cosine of the static contact angle at the centre of the droplet,

$$F_\theta(x_G,t) = \frac{\pi\gamma_{lv} R(x_G,t)}{2} \left[\cos\theta_a(x_G + R(x_G,t)) - \cos\theta_r(x_G - R(x_G,t))\right]. \quad (7)$$

Finally, Eq. 7 shows the link between CAH and the driving force. When the rim is moving, the contact angle at the front is called the advancing contact angle and at the rear, the receding contact angle.

As mentioned, the viscous force balances the driving force since the inertial term has proven to be negligible [4]. There are several studies regarding this viscous force, especially how to take into account the singularity near the contact line region [2, 6]. Subramanian et al. [6] proposed the viscous force model chosen in this study. Considering the lubrication theory, a Poiseuille type velocity profile in the droplet and a geometrical relation between the footprint radius of the droplet and the real contact angle, they established:

$$F_\mu(x_G,t) = -6\pi\mu U(x_G,t)R(x_G,t) \left(g(\theta,1-\varepsilon) - g(\theta,0)\right) \quad (8)$$

with,

$$g(\theta,\xi) = -[\cot\theta(x_G,t)\ln(\sqrt{\csc^2\theta(x_G,t)-\xi^2} - \cot\theta(x_G,t)) + \sqrt{\csc^2\theta(x_G,t)-\xi^2} - \cot\theta(x_G,t)]. \quad (9)$$

The viscous force implicitly displays the slip length term L_s. The slip length is directly related to parameter ε by the relation $L_s = \varepsilon R(x_G, t)$. It corresponds to the length at which the description of the physical phenomena at the macro scale is no longer valid. This parameter has been widely studied in the literature [2, 7, 8]. An *a posteriori* analysis of the effect of this parameter showed that the model is not sensitive to the slip length for a range of $10^{-10} < L_s$ (m) $< 10^{-9}$. So, the value of $0.5\text{x}10^{-9}$ m was chosen.

2.3 Results and discussion

As mentioned previously, Moumen et al. [4] prepared three different gradient intensities labelled "weak", "intermediate" and "sharp". The data were fitted by a sigmoidal, logistic four-parameter function (see Fig. 2).

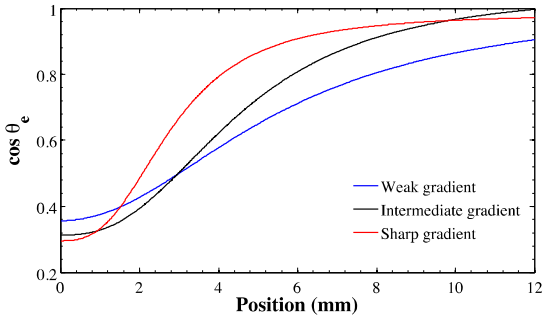

Fig. 2 Sigmoidal, logistic four-parameter function representing the cosine of the contact angle θ_e on the three different wettability gradients plotted against the position along the gradient surface. The working fluid is tetraethylene glycol.

The results presented below concern the intermediate gradient and a drop volume of 500 nL. The working fluid was tetraethylene glycol. As stated previously, Moumen et al. developed a model for accommodating the measured and predicted velocities. Their method consists in subtracting the equivalent force due to hysteresis effect, at a given location, using a critical footprint radius that they found experimentally. They reached a good agreement between the measured and predicted velocities in the deceleration phase of the trajectory. In the acceleration phase, the driving force was still overestimated.

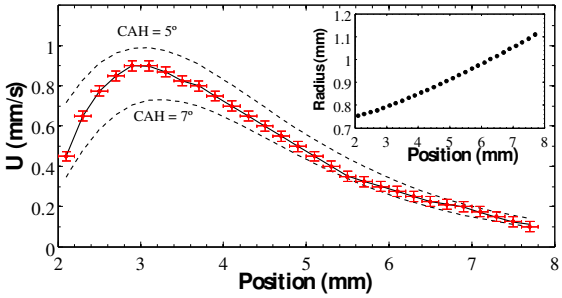

Fig. 3 Comparison between measured and calculated velocities for a 500 nL volume droplet of tetraethylene glycol placed on the intermediate gradient. The filled diamonds correspond to the experimental data extracted from [4], the dashed curves represent the model with a constant CAH, while the solid line stands for the same model adjusting CAH to match the experimental and calculated velocities. The inset displays the footprint radius plotted against the position.

In the present model, we used a constrained least-square optimization method in which the local CAH was the adjustable parameter, managing to accommodate the experimental and predicted velocities (Fig. 3). The trajectories with two homogeneous CAH (5° and 7°) are plotted in Fig. 3. The model appears to be more sensitive to the CAH during the acceleration phase, which could explain why the model established by Moumen et al. [4] had some difficulties to accommodate the driving force. The inset plot in Fig. 3 shows the variation of the footprint radius of the droplet. The radius increases from 0.75 mm to 1.11 mm with position due to the decrease of the real contact angle (spreading effect). The contact angle hysteresis at each location is found in order to accommodate the data as shown in Fig. 4. This space dependence can be attributed to the chemical and roughness heterogeneities of the surface. The CAH calculated to adjust the experimental velocities varies from 5° to 7° for the 500nL volume droplet of tetraethylene glycol. This result seems to be in agreement

with typical CAH values in the literature. Actually, Daniel and Chaudhury [9] report a similar CAH using the same chemical treatment as Moumen et al. [4].

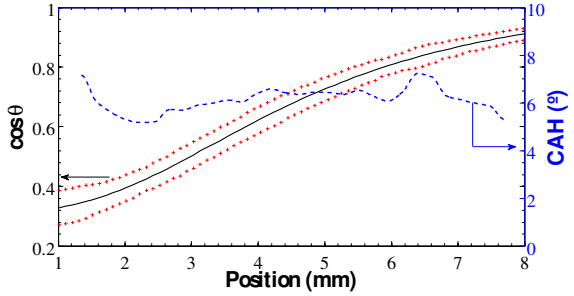

Fig. 4 The black curve represents the cosine of the equilibrium angle as a function of position that has been characterized by a sigmoidal, logistic function [4]. The curve drawn in crosses corresponds to the cosine of the CAH function that best adjusts the experimental data and dot line curve represents the CAH function itself. The volume of the droplet is 500nL and $L_s = 0.5x10^{-9}$m.

Therefore, the model is able to predict the trajectories of several droplets as presented in the following figure (Fig. 5). The different *CAH (x)* functions show that even though the mean value of all the CAH is found to be reasonable regarding the literature (comprised between 4.4º and 6.7º), spatial heterogeneities must be taken into account for rigorous prediction of the trajectory.

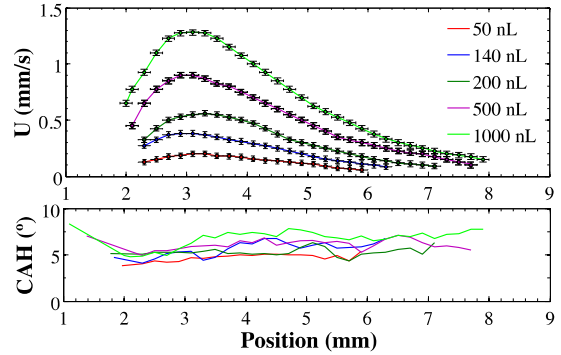

Fig. 5 Comparison between the measured [4] and calculated velocity profiles for different nominal volumes of droplets for $L_s = 0.5x10^{-9}$ m. For each curve there is a corresponding identified *CAH (x)* function allowing to match the experimental and calculated velocities. 50, 140, 200, 500 1000 nL are represented by red, blue, dark green, pink and light green curves respectively.

3. Model analyses

In this section, two specific analyses are developed. The first concerns the effect of contact angle hysteresis using the intermediate wettability gradient surface of Moumen et al. [4]. In the second part, the critical footprint radius corresponding to the onset of motion of a droplet is determined according to the surface properties and the droplet parameters.

3.1 CAH effect

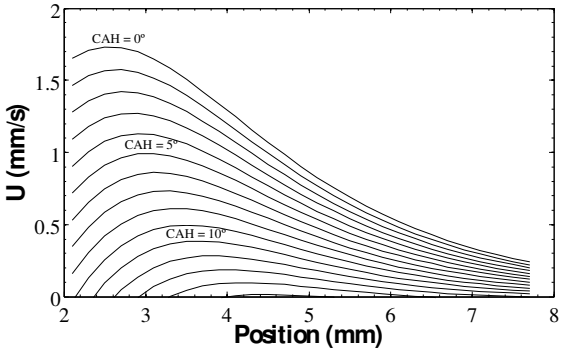

Fig. 6 Different velocity profiles plotted against position considering CAH varying from 0º to 14º. Effect of CAH to a droplet trajectory of 500 nL volume on the intermediate gradient ($L_s = 0.5x10^{-9}$m).

Fig. 6 shows the influence of the CAH on the velocity of a droplet of 500 nL placed on the intermediate gradient of Moumen et al. We assumed homogeneous CAH between 0º and 14º. The latter value corresponds to the highest value of the CAH for which a motion of the droplet can be obtained. Results also show that for high CAH, the droplet must be placed farther in the gradient in order to obtain motion. Finally, the higher the CAH, the lower the maximum value reached by the velocity. This behaviour was found to be the same whatever the gradient (weak, intermediate and sharp).

3.2 Critical radius

Moumen et al. [4] established a critical footprint radius empirically, which represents the size at which the droplet moves considering a known wettability gradient. Below, we mathematically determine an expression of this critical radius considering a

single droplet placed on an upward inclined surface with a wettability gradient. Before the onset of the motion, there are two opposite forces that equilibrate the droplet: the driving force F_θ (Eq. 7) and gravity F_g. Therefore, there are two obvious solutions for the movement of small droplet in Eq. 1:

- $F_\theta > |F_g|$ the droplet runs uphill,
- $F_\theta < |F_g|$ the droplet runs downhill.

Replacing both expressions of driving and gravity forces in Eq. 1 we obtain:

$$\left[\cos\theta_a(x_G+R)-\cos\theta_r(x_G-R)\right] - \frac{2}{3}R^2\frac{g\rho_l}{\gamma_{lv}}f(\theta)\sin\alpha = 0 \quad (10)$$

where,

$$f(\theta) = \frac{2-3\cos\theta(x_G,t)+\cos^3\theta(x_G,t)}{\sin^3\theta(x_G,t)}. \quad (11)$$

It can be seen in Eq. 10 that the capillary length appears:

$$L_{cap} = \sqrt{\frac{\gamma_{lv}}{g\rho_l}}. \quad (12)$$

Assuming that the cosine of the static contact angle evolves linearly with the position ($a_a = a_r = a$ and b_a, b_r the slope and intercept of the advancing and receding cosine function, respectively), Eq. 10 then becomes a 2nd order polynomial function of the footprint radius:

$$-\frac{2}{3L_{cap}^2}f(\theta)\sin\alpha R(x_G,t)^2 + 2aR(x_G,t)+b_a-b_r = 0. \quad (13)$$

Therefore, there are two critical radius solutions for Eq. 13. As shown in Fig. 7, the first critical radius R_1 represents the size of the droplet from which motion is upward (for $R_2 > R > R_1$ then $F_\theta > F_g$) considering an inclination α, a wettability gradient slope a and a known homogeneous CAH. The second solution R_2 of the second-order polynomial equation stands for the size at which the drop begins to slide backward (for $R > R_2$ then $F_\theta < F_g$). For $R < R_1$, the CAH pins the droplet so there is no motion.

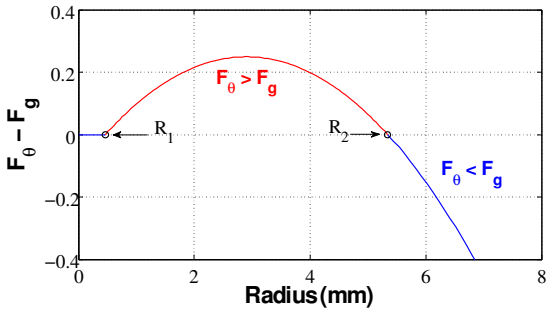

Fig. 7 Determination of the critical radius that allows the droplet to be set in motion. The parabola corresponds to the second-order equation (Eq. 13) for a wettability gradient slope a = 0.12 mm^{-1}, an inclination of α = 15° and a CAH = 5°.

The results presented below correspond to a droplet of tetraethylene glycol with a capillary length L_{cap} = 2.0416 mm where the liquid-vapour tension is γ_{lv} = 0.046 $N.m^{-1}$, the density ρ_l = 1125 $Kg.m^{-3}$ and the gravitational constant g = 9.81 $m.s^{-2}$. The main hypothesis of the present work is that the droplet remains in its spherical cap shape during the displacement. This assumption is verified when Eq. 13 and the relation Bo << 1 are met. In the following results with tetraethylene glycol, when R >> R_2, the previous assumption is not verified, so the model might not be conclusive for this radius range. Several plots can then be derived to show the impact of the three parameters α, a and CAH on setting the droplet in motion.

Fig. 8 represents Eq. 13 plotted against the footprint radius for different inclination angles. When α = 0°, Eq. 13 becomes an affine equation and there is just one footprint radius solution: the critical footprint radius defined in [4] and previously in [10]. Moreover, it can be seen that the steeper the inclination the greater the footprint radius has to be in order for the droplet to move upward. Nevertheless, near 60° the droplet only moves downhill due to gravity on the wettability gradient used (a = 0.12 mm-1) and CAH = 5°. The following plot (Fig. 9) represents the influence of the wettability gradient slope. As predictable, the stronger the intensity of the gradient, the smaller the footprint radius found as a solution of Eq. 13. We can also note that the footprint

radius R_2 increases with the intensity of the gradient, which means that a sharper gradient is capable of driving greater droplet volumes.

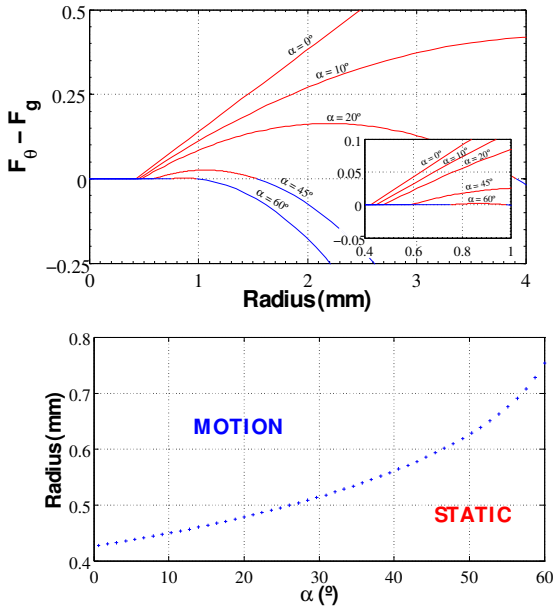

Fig. 8 Effect of the inclination angle α to the critical footprint radius R_1. The slope of the wettability gradient is a = 0.12 mm^{-1}, CAH = 5º and $\theta(x_G, t) = 67.5º$.

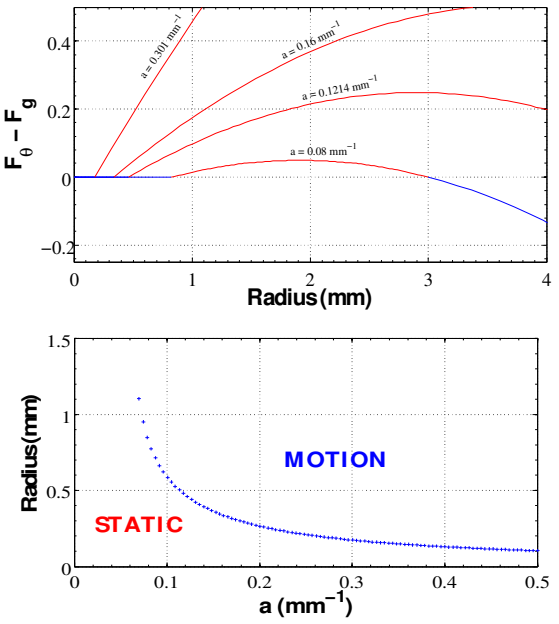

Fig. 9 Effect of the wettability gradient intensity on the critical footprint radius R_1. The inclination of the plane is α = 15º, CAH = 5º and $\theta(x_G, t) = 67.5º$.

Finally, Fig. 10 shows the impact of the CAH on the critical footprint radius of the droplet. Once again the model shows that the hysteresis effect prevents the droplet from moving. The footprint radius increases with the CAH, which means that for high values of CAH, the droplet has to be greater to move uphill in a given wettability gradient. However, the model predicts a maximum value of CAH equivalent to 20º from which upward motion is no longer possible (for α = 15º and a wettability gradient slope a = 0.12 mm^{-1}).

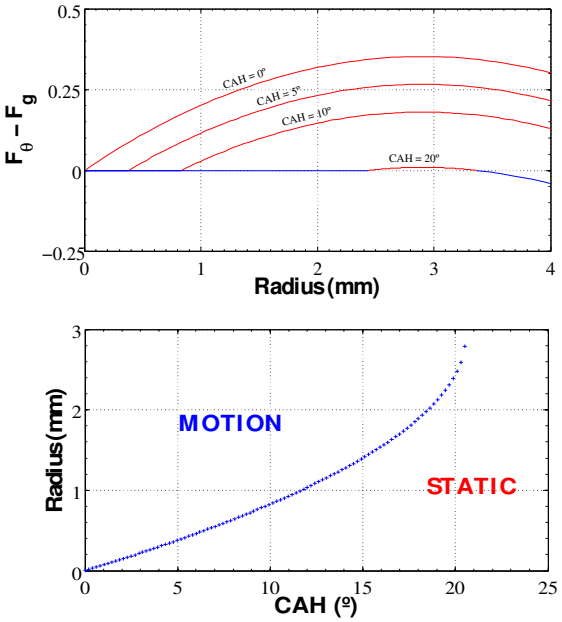

Fig. 10 Effect of the CAH on the critical footprint radius R_1. The wettability gradient is a = 0.12 mm^{-1}, the inclination of the plane is α = 15º and $\theta(x_G, t) = 67.5º$.

4. Conclusion and perspectives

The work presented in this paper shows the dynamics of a small droplet placed on an inclined plane with a wettability gradient on the surface. A new model of the driving force due to the gradient on the surface is presented. Unlike many others, this model explicitly takes into account the local CAH. The model was used with experimental data extracted from the open literature. Experimental and predicted velocities are in very good agreement considering a reasonably heterogeneous CAH profile. Secondly, the model was used to find the so-called critical footprint radius, in others words, to know what footprint radius, i.e. nominal volume, the droplet must have in order to start moving upward on an inclined plane, considering a

given wettability gradient and CAH. The analyses and results show that CAH is a key parameter in the accurate prediction of the droplet dynamics. The results obtained in this study strongly support the need for future work to experimentally reproduce the critical footprint radius.

Acknowledgements

This work was funded by the European Space Agency, Microgravity Application Program "MANBO" (Multiscale ANalyses BOiling).

References

[1] H.P. Greenspan, On the motion of a small viscous droplet that wets a surface. Journal of Fluid Mechanics Vol. 84, 125 (1978)

[2] F. Brochard, Motions of droplets on solid surfaces induced by chemical or thermal gradients. Langmuir, Vol. 5, 432-438 (1989)

[3] M.K. Chaudhury and G.M. Whitesides, How to make water run uphill, Science, Vol. 256, 1539-1541 (1992)

[4] N. Moumen, R.S. Subramanian and J.B. McLaughlin, Experiments on the motion of drops on a horizontal solid surface due to wettability gradient, Langmuir, Vol. 22, 2682-2690 (2006)

[5] T. Young, An essay on the cohesion of fluids. Philosophical Transactions of the Royal Society of London, Vol. 95, 65-87 (1805)

[6] R.S. Subramanian, N. Moumen and J.B. McLaughlin, Motion of a drop on a solid surface due to wettability gradient, Langmuir, Vol. 21, 11844-11849 (2005)

[7] P.G. de Gennes, Wetting: Statics and dynamics. Rev. Mod. Phys., Vol. 57, 827-863 (1985)

[8] P.G. de Gennes, F. Brochard-Wyart and D. Quéré, Gouttes, bulles, perles et ondes. Collection échelles, Bélin (2005)

[9] S. Daniel and M.K. Chaudhury, Rectified motion of liquid drops on gradient surfaces induced by vibration, Langmuir, Vol. 18, 3404-3407 (2002)

[10] S. Daniel, M.K. Chaudhury and J.C. Chen, Fast drop movements resulting from the phase change on a gradient surface, Science, Vol. 291, 633-636 (2001)